J Mater Sci: Mater Med (2010) 21:1573–1586
DOI 10.1007/s10856-010-3997-5

Investigation on magnetically controlled delivery of doxorubicin from superparamagnetic nanocarriers of gelatin crosslinked with genipin

Jyoti Choubey · A. K. Bajpai

Received: 13 October 2009 / Accepted: 8 January 2010 / Published online: 5 February 2010
© Springer Science+Business Media, LLC 2010

Abstract Gelatin (Type B) nanoparticles were prepared by a single W/O emulsion technique and characterized by infrared (IR) spectra, transmission electron micrographs (TEM), surface potential measurements and magnetization studies. Whereas the IR spectra clearly confirmed the presence of gelatin, genipin and doxorubicin in the loaded nanoparticles, the transmission electron micrographs (TEM) image depicts smooth surface, spherical shape and non-uniform size of nanoparticles (up to 100 nm). The prepared nanoparticles were loaded with doxorubicin, a well known anticancer drug, and in vitro release dynamics of entrapped drug was investigated as a function of various experimental factors such as percent loading of the drug, chemical architecture of the nanocarriers, and pH, temperature, ionic strength and nature of the release medium in presence and absence of magnetic field. The nanoparticles were also studied for their water sorption capacity. The drug release process was analyzed kinetically using Ficks power law and a correlation was established between the quantity of released drug and swelling of the nanoparticles.

1 Introduction

Cancer is characterized by a reduction or loss of cellular control and normal maturation mechanisms. Its features include excessive cell growth, undifferentiated cells and tissues, and the ability to grow into neighboring tissues and to metastasize. The choice of treatment includes the total excision of tumor tissue and possibly part of the adjacent tissues, combination chemotherapy, immunotherapy, radiation treatment, and a combination of these. Since complete eradication of cancer cells is imperative for successful treatment, total excision is the treatment of choice if applicable. However, depending on the location and the involvement of the tumor with surrounding tissues, surgery may not always be possible. Under such circumstances radio- or chemotherapy becomes necessary. However, severe complications with these treatments have been reported. Therefore, the development of techniques that could selectively deliver drug molecules to the diseased site, without a concurrent increase in its level in the healthy tissues of the organism, is currently one of the most active areas of cancer research [1].

In the past, chemotherapy targeted by magnetic fields using magnetic albumin microspheres has shown encouraging results [2].

Targeting and prolonged retention of the Ferro fluids complex at the target site reduces its reticuloendothelial system (RES) clearance and facilitates extra vascular uptake. To optimize intratumoral magnetic particle concentration, several features need to be considered: (*a*) the particles should be of a size that allows sufficient attraction by the magnetic field and their introduction into the tumor or into the vascular system surrounding the tumor; (*b*) the magnetic fields should be of sufficient strength to be able to attract the magnetic nanoparticles into the desired area; (*c*) the FF complex should deliver and release a sufficient amount of anticancer agent; and (*d*) the method of injection should have good access to the tumor vasculature and should avoid clearance by the reticuloendothelial system ("first pass effect") [3].

J. Choubey · A. K. Bajpai (✉)
Bose Memorial Research Laboratory, Department of Chemistry, Government Autonomous Science College, Jabalpur 482 001, India
e-mail: akbmrl@yahoo.co.in; akbajpailab@yahoo.co.in
URL: www.sciencecollegejbp.org

Numerous studies have been performed to magnetic field as guiding force to deliver drugs. For instance, Collagen gels (1 cm thick) were prepared with magnetite (10 nm) for the release of rhodamine-labeled dextran (Dex-R) using an oscillating magnetic field. Magnetic field release studies were performed in phosphate buffer solution for up to four days with a magnetic field strength of 14,000 G and frequency of 0.3 Hz [4].

Polyelectrolyte microcapsules (5 μm) made of poly (sodium styrene sulfonate) (PSS) and poly (allylamine hydrochloride) (PAH) bilayers containing ferromagnetic gold-coated cobalt (3 nm) were synthesized to uptake FITC-dextran in order to determine permeability, a transport phenomenon similar to release [5].

Nickel ferrite particles (5–8 nm) coated with poly (methacrylic acid) (PMAA) was created to release the anticancer drug doxorubicin (Dox). A magnetic field of 1000 Oe was applied for release studies for up to 10 days. Higher release of Dox was found in the presence of the magnetic field than in its absence [6].

There are several types of magnetic materials that can be controlled by magnetic fields for drug release applications, along with others biomedical applications. Commonly used magnetic substances include stainless steel magnetic alloy [7]; various cobalt particles including cobalt ferrite ($CoFe_2O_4$) [8], gold coated cobalt (Co@Au) [5], and samarium cobalt [7]; and the family of iron oxides, including nickel ferrites [7], hematite (Fe_2O_3), maghemite (γ-Fe_2O_3) [9], and magnetite(Fe_3O_4).

Magnetite (Fe3O4) nanoparticles that have excellent magnetic saturation (−78 emu/g) are desirable for these applications due to the strong ferromagnetic behavior, less sensitivity to oxidation and relatively low toxicity compared to many other materials (e.g., iron, nickel and cobalt) [10]. These magnetite nanoparticles can be produced by co-precipitation of iron (II) and iron (III) chloride salts in the presence of ammonium hydroxide at pH 9–10, and can be easily stabilized by oleic acid in nonpolar solvents [11]. Magnetite has also been known to have low toxicity [12].

Biodegradable polymers can be used as temporary implants that are needed to hold their structure for a limited time, such as with absorbable sutures and staples, cell scaffolding for bone regeneration [13], gene delivery [14], and drug delivery systems [15]. Common biodegradable polymers used in many of these applications include poly (lactic co-glycolic acid) (PLGA) [24, 25], poly (ethyl-2-cyanoacrylate) (PECA) [16], poly (ε-caprolactone) (PCL) [17], poly (ethylene oxide) (PEO) [18], poly(ethylene glycol) (PEG) [19], collagen [4], and alginate [20].

Use of the nanoparticles for any biomedical applications is largely dependent on their physiological characteristics. Selecting a suitable modifier that mimics physiological condition is essential to protect these nanoparticles from aggregation and coalescence. Gelatin is derived from collagen and is commonly used to immobilize drugs and genes to produce controlled released products for pharmaceutical and medical applications [21].Gelatin, being water soluble, biodegradable, and biocompatible, can also be one promising candidate for the surface modification of iron oxide [22].

Gelatin microspheres have been widely evaluated as a drug carrier. Nevertheless, gelatin dissolves rather rapidly in aqueous environments, making the use of the polymer difficult for the production of long-term delivery systems. This adverse aspect requires the use of a crosslinking agent in forming insoluble networks in microspheres. However, the use of crosslinking agents such as formaldehyde and glutaraldehyde can lead to toxic side effects owing to residual crosslinker. In an attempt to overcome this problem, a naturally occurring crosslinking agent (genipin) was used to crosslink gelatin microspheres as a biodegradable drug-delivery system for intramuscular administration [23].

Much effort in research is directed toward finding less toxic and more efficient pharmaceutical formulations, especially for anticancer drugs. Conjugating some drugs to colloidal carriers has been shown to favorably influence their efficacy and toxicity [24]. For example, doxorubicin (DOX), known for its cardiotoxicity, bone marrow and gastrointestinal toxicity [25] was shown to be less toxic when associated with nanoparticles [26].

In the present work a novel strategy for combined cancer therapy by employing iron-oxide incorporated gelatin nanoparticles (IOIGNP) as a drug-delivery carrier is reported. In the current study undertakes to produce and characterize doxorubicin-loaded (Dox; an anticancer drug) iron oxide incorporated gelatin nanoparticles as a novel drug delivery system for magnetically controlled release of anticancer drug.

2 Theory of magnetisation

It is assumed that magnetic nanocomposite particles that display high saturation magnetization have potential applications for magnetically controlled drug targeting. These particles (in the range of 10 nm to a few microns) are relatively magnetic with discrete randomly oriented magnetic moments. When the magnetic particles are placed in an external field, the moments of the particles rapidly rotate into the direction of the field and improve the magnetic flux density. To control the motion of such particles within a circulation system, a magnetic force due to an externally applied magnetic field and a hemodynamic drag force due to the fluid flow combine to create a total vectoral force on the particles. In order to effectively overcome the influence of a fluid flow and achieve the

desired external magnetic field-controlled guidance, the magnetic force because of the external field must be larger than the drag force or hydrodynamic force. According to this explanation, the magnetic force on the magnetic particles is governed by [10, 27]:

$$\vec{F} = \vec{\nabla}\left(\vec{m} \cdot \vec{B}_0\right) \quad \text{(Newtons)}, \tag{1}$$

where F is the magnetic force, m is the total magnetic moment of the material in the microspheres, r is the gradient that is assumed to be derived from characteristics of the field alone, and Bo is the magnetic flux density—also known as the Bo field. Each of these quantities thus influences the some degree to which an external magnetic field may be used to internally guide particles in the body. The del operator r; is defined for a magnetic field distribution at xyz directions [28]

$$\nabla \equiv \frac{\partial}{\partial x} a_x + \frac{\partial}{\partial y} a_y + \frac{\partial}{\partial z} a_z. \tag{2}$$

It is noted that the gradient of a scalar function at any point is the maximum spatial change of the magnetic field. The B0 field tends to align the net magnetic moment of the particle in a fixed direction while the gradient leads to a force that may move the particles.

The second factor characterizes the magnetic properties of the particles. The magnetic moment of a material m is proportional to the applied magnetic field H, and the intrinsic magnetic susceptibility of the material, χ_m [28]:

$$m = \chi_m H. \tag{3}$$

The force that counteracts the magnetic force on the particle in the fluid stream is due to the liquid (e.g., blood) flow. Stokes Law governs the hemodynamic forces on a particle in the liquid [29]:

$$F = 6\pi\eta\upsilon r, \tag{4}$$

where F is the drag force, η is the viscosity of a fluid, v is the relative velocity of a spherical particle, and r is the radius.

2.1 Experimental

2.1.1 Materials

Acid processed gelatin (Type A, isoelectric point 7.6) in yellowish granular form, was supplied by Loba Chemie, Mumbai, India and used without any pretreatment. Type B gelatin (Bloom No. 240, isoelectric point 4.8) extracted from human bone was a kind gift from Shaw Wallace Gelatins Ltd., Jabalpur, India. Genipin was employed as a crosslinker of gelatin and obtained from Wako Chemicals Japan. Parafin oil was used as oil phase. Other chemicals and solvents were of analytical reagent grade. Doxorubicin (DOX) was used as a model drug and obtained from Daber Pharma LTD.

2.2 Methods

2.2.1 Preparation of nanoparticles

The preparation methods of nanoparticles for pharmaceutical use are divided broadly into two categories, those based on physicochemical properties such as phase separation [30] and solvent evaporation [31], and based on chemical reactions such as polymerization and polycondensation. In the present study, solvent evaporation technique has been followed. Briefly, the method may be described as below:

For the preparation of the nanoparticles gelatin (5, 8 and 11 wt%) was first dissolved in 40 ml deionized water at 45 0C to ensure its complete dissolution. For preparing the oil phase 80 ml paraffin oil was used The above two solutions were mixed with vigorous shaking (Shaking speed 300 RPM, 0.5 HP Motor Capacity) (Toshniwal, India) for 30 min and to this suspension with constant shaking was added genipin emulsion (with different weight ratio i.e., 0663, 0.1326, 0.1989 mM concentration) prepared in 9 ml ethanediol and 1 ml paraffin oil. The crosslinking reaction was allowed to take place for predetermined time period. Nanoparticles so prepared were cleaned by centrifuging and re-suspending in toluene three times and then twice in acetone. The final product was dried at room temperature to obtain a fine bluish powder which was stored in air tight polyethylene bags.

2.2.2 Impregnation of Iron Oxide into the nanoparticles

For synthesis of iron oxide nanoparticles the solution of Fe ions was prepared from $FeCl_2{\cdot}4H_2O$ and $FeCl_3{\cdot}6H_2O$ salts ($Fe^{2+}/Fe^{3+} = 0.5$) in acidic condition by continuous stirring the solution for 0.5 h under nitrogen atmosphere at room temperature. A solution of 10% NH_4OH was added dropwise into the solution of Fe ions to precipitate nanoparticles of iron oxide according to the reaction given below:

$$2FeCl_3 + FeCl_2 + 8NH_4OH \rightarrow Fe_3O_4 + 8NH_4Cl + 4H_2O \tag{5}$$

The precipitated iron oxide nanoparticles were filtered and repeatedly washed with distilled water.

The change in color of the particles turns from bluish to dark red brown which also confirm the formation of oxides of iron as shown in Fig. 1a and b. Mechanism of incorporation of iron oxide onto the nanoparticles surface is shown in Fig. 2.

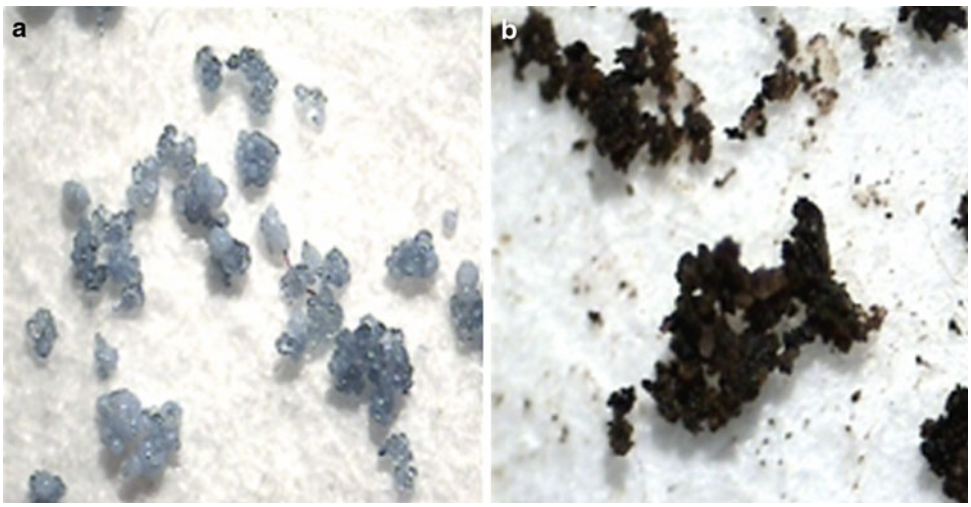

Fig. 1 An optical microscopic photograph of genipin cross linked gelatin-nanoparticle (**a**) and iron oxide incorporated gelatin nanoparticles (**b**)

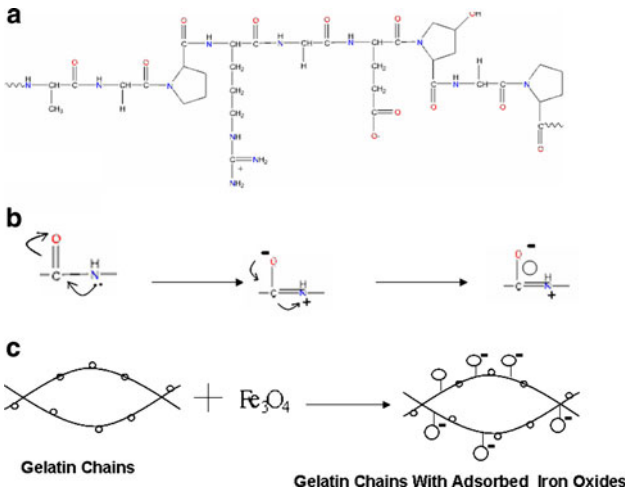

Fig. 2 A reaction scheme of depicting the incorporation of iron oxide onto the gelatin nanoparticles

In aqueous system, iron oxide incorporated gelatin nanoparticles (IOIGNPS) are coordinated with water molecules, which share their electron pairs with iron atom. Upon adsorption, the water molecules usually dissociate resulting in a surface covered by hydroxyl groups coordinated to the underlying iron atoms [32]. The hydrous iron oxides have amphoteric characteristics that can act as positive($FeOH^{+2}$) site and interact with lone pair of electrons present in nitrogen atoms of amine groups and/or anionic carbonyl oxygen in acidic medium [33, 34] or act as negative (FeO^{-}) site and interact with electron deficient groups in basic or neutral medium [32]. In the present study, the IOIGNPS were washed to neutral pH and no acidic solution was used, negative FeO^{-} site can be expected on the surface of the IOIGNPS. Furthermore, gelatin being a protein is made up of amino acids Fig. 2. Each of the amino acids is joined by peptide bonds between the carbonyl and amino groups of adjacent amino acid residue forming a linear chain. The linear chains are held together by H-bond leading to formation of complex secondary and tertiary structure [35]. Due to electron withdrawing nature of carbonyl group in each amino acid groups, the lone pair of electron on the nitrogen atom is delocalized by resonance, thus forming a partial double bond with the carbonyl carbon and putting a negative charge on the oxygen and positive charge on the nitrogen atom.

2.3 Swelling experiments

The extent of swelling of nanoparticles was determined by a conventional gravimetric procedure. In a typical experiment, preweighed nanoparticles (with iron oxide) were allowed to swell in distilled water for a predetermined time period (up to equilibrium swelling) and thereafter the particles were taken out from the water and gently pressed in-between the two filter papers to remove excess of water and finally weighed using a sensitive balance (APX–203 Denver, Germany).A time period of 24 h was found to be enough for equilibrium swelling. The swelling ratio was determined by the following Eq. 6.

$$\text{Swelling ratio } (S_r) = \frac{\text{Weight of swollen nanoparticles } (w_a)}{\text{Weight of dry nanoparticles } (w_d)} \quad (6)$$

Table 1 Data showing the influence of composition of the nanoparticles on the equilibrium swelling and percent impregnation of iron oxide

S. no	Paraffin oil (ml)	Gelatin (g)	Genipin (mg)	Equilibrium swelling
1	80	5	0.015	4.28
2	80	5	0.030	4.33
3	80	5	0.045	3.00
4	80	11	0.045	1.46
5	80	8	0.045	2.82

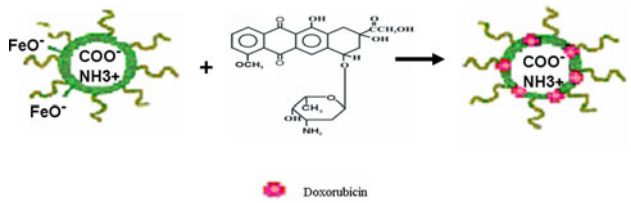

Fig. 3 Schematic presentation of loading of drug molecule onto the iron oxide incorporated nanoparticles

The amount of water sorption by the sample provides information about the hydrophilic nature of the material. Swelling results are summarized in the Table 1.

The preparation of doxorubicin-loaded (Dox; an anticancer drug) IOIGNP is shown schematically in Fig. 3. Doxorubicin-loaded (Dox; an anticancer drug) IOIGNP bearing carboxyl groups in the polymer coating layers were synthesized as described previously. It is supposed that Dox could be incorporated in the polymeric IOIGNP through electrostatic interactions between positively charged Dox and the negatively charged FeO^- and COO^- coating layers.

3 Characterisation

3.1 FTIR spectra

The FTIR spectra of gelatin nanoparticles and drug loaded nanoparticles were recorded on a FTIR spectrophotometer (Shimadzu 8201 PC).

3.2 Electron microscopy study

The morphological features of the nanocomposites and iron oxide particles were investigated by recording transmission electron micrographs (TEM) (Hitachi Hu-11 B), respectively.

3.3 Surface potential measurements

In order to understand the nature of the drug doxorubicin (DOX)-nanoparticle interaction surface potential studies were performed with a digital pH meter (Systronics Model No. Digital pH Meter MK VI, Ahamadabad, India). In a typical experiment 0.2 g nanoparticle were dispersed into 20 ml of respective pH solution and emf was recorded using a compound electrode system. A similar experiment was also repeated for drug loaded nanoparticles.

3.4 Magnetization measurements

Magnetic properties of nanocomposite particles were characterized by a Quantum Design (USA),14T PPMS Vibrating Sample Magnetometer (VSM).

3.5 Loading of doxorubicin (DOX)

For loading of nanoparticles, known volume of drug injections were taken and diluted with appropriate amount of phosphate buffer saline and shaken vigorously for mixing of drug injection and distilled water.

The loading of DOX was performed by allowing the nanoparticles to swell in the freshly prepared drug solution till equilibrium, and then drying to obtain the release device. The percent loading of drug was calculated by the following eq.

$$\% \text{ Loading} = \frac{W_d - W_O}{W_O} \times 100 \quad (7)$$

where W_d and W_o are the weights of loaded and unloaded nanoparticles, respectively.

3.6 In vitro release experiment

Release experiments were performed in phosphate buffer saline (PBS) (pH 7.4, 1.2 mM KH_2PO_4, 1.15 mM Na_2HPO_4, 2.7 mM KCl, 1.38 mM NaCl) in presence of magnetic field(25, 75.150 and 225 gauss). In order to determine the released amount of the doxorubicin (DOX), into 0.1 g of drug-loaded nanoparticles was added 8 ml of phosphate buffer saline (PBS) as a release medium (pH 7.4) and the resulting suspension was gently shaken for predetermined time period. After shaking was over, 3 ml of supernatant was withdrawn and 3 ml supernatant was withdrawn assayed for DOX spectrophotometrically.

3.7 Kinetics of release process

For monitoring the progress of the release process, 3 ml of aliquots were withdrawn at desired time intervals and instantly replaced by fresh release medium (PBS). In the aliquots withdrawn, the amount of DOX was determined as described above.

For achieving mechanistic insights into the release process of DOX, the following equation was used [36],

$$\frac{W_t}{W_\infty} = k\, t^n \quad (8)$$

where W_t/W_∞ is the fractional release at time t and k is rate constant. The exponent n, called as diffusional exponent, is an important indicator of the mechanism of drug transport and, in general, has a value between 0.5 and 1. When $n = 0.5$, the release is taken to be Fickian. When $n = 1$, the release is zero order (Case II transport), and in between these values, i.e., $0.5 < n < 1$, the release is described as anomalous. When $W_t/W_\infty = 0.5$, t is the half life, another extremely useful parameter in comparing systems.

3.8 Chemical stability of drug

Chemical stability of drug in acidic media (pH—1.8) was judged by UV spectrophotometric method (Double Beam UV-vis Spectrophotometer—2201, Ahamadabad, India) as explained elsewhere [37].

4 Results and discussion

4.1 Characterization of nanoparticles

4.1.1 FTIR spectral analysis

The FTIR spectra of genipin cross linked nanoparticles and drug loaded iron oxide incorporated nanoparticles are shown in Fig. 4 a and b, respectively which clearly confirm the presence of gelatin, genipin, iron, and drug in nanoparticles. The strong band observed at 2928 cm^{-1} due to C–H stretching confirms the presence of methyl group. The band observed at 1524 cm^{-1} due to N–H bending vibration confirms the presence of primary amine in gelatin molecule. A band at 1444 cm^{-1} due to ring stretching vibrations confirms the presence of dihydropyrane ring (Heterocyclic ring) in the genipin (Fig. 4a).

A band observed at 1683 cm^{-1} due to C=N stretching confirms the presence of amine. A band at 1521 cm^{-1} due to N–H stretching of gelatin. A band at 1460 cm^{-1} due to ring stretching vibrations confirms the presence of heterocyclic ring in the drug molecule. The presence of iron oxide in the hydrogel is evident from the absorption bands appeared in the region between 450 and 480 cm^{-1} [38] and they may be assigned to Fe–O bonds of magnetite.

Electron Microscopy

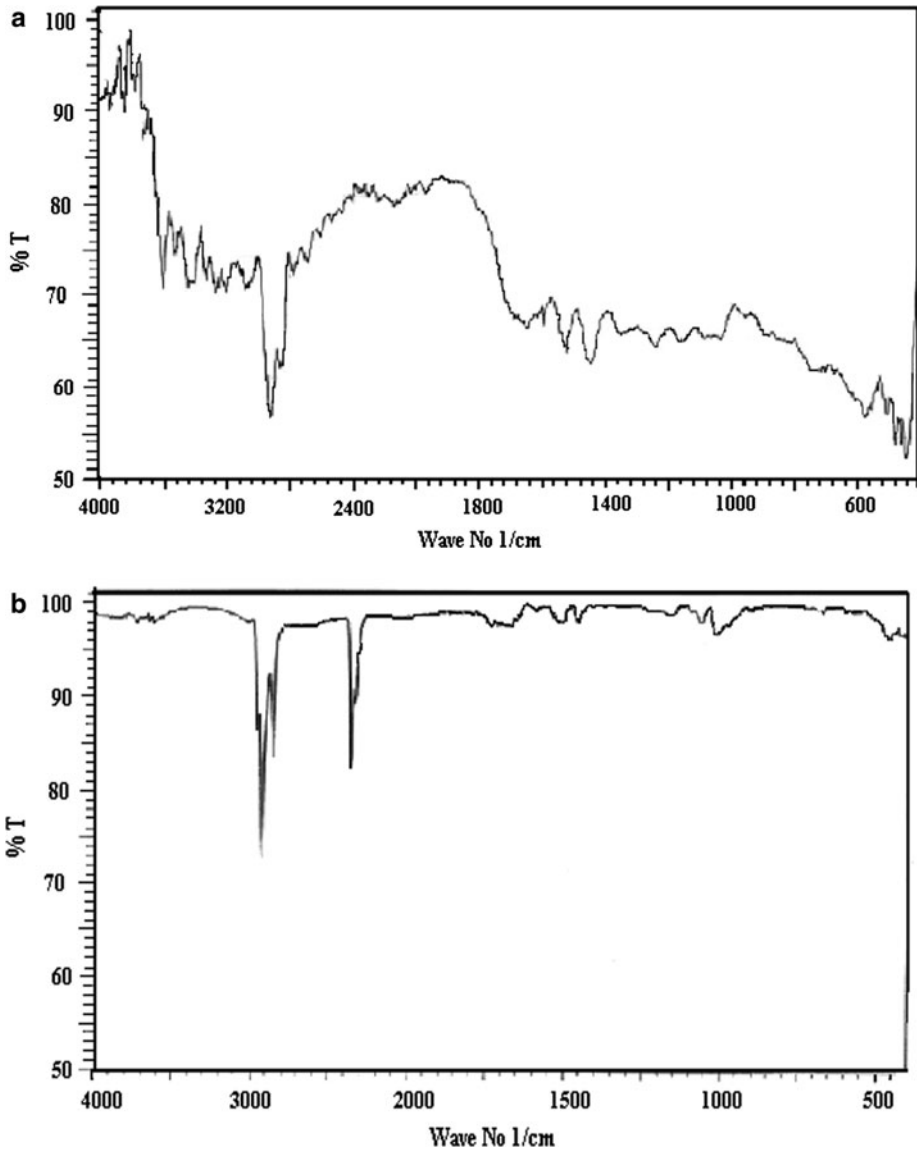

Fig. 4 FTIR spectra of **a** genipin crosslinked native gelatin nanoparticles, and **b** iron oxide incorporated doxorubicin-loaded gelatin nanoparticles

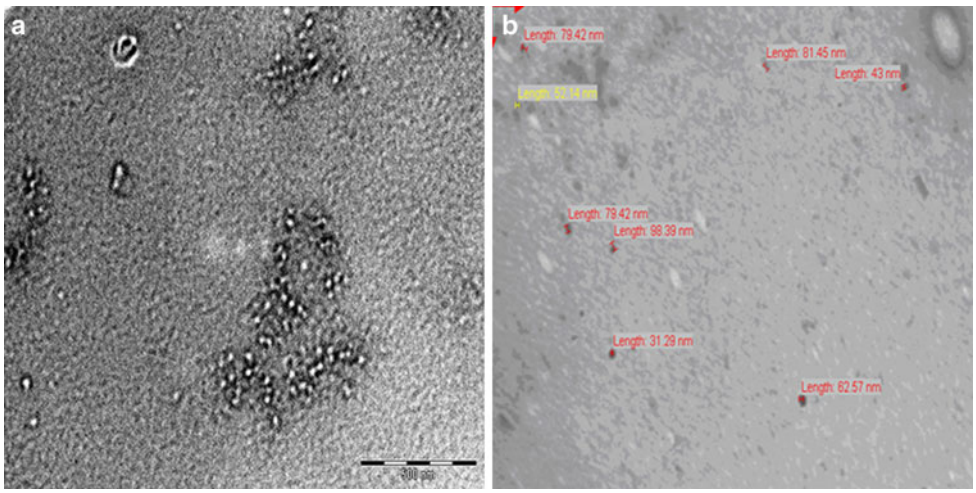

Fig. 5 Transmission electron micrographs (TEM) of **a** genipin crosslinked gelatin nanoparticles and **b** iron oxide-loaded nanoparticles

The morphological features of the prepared impregnated nanoparticles have been investigated by TEM analysis of iron oxide incorporated nanoparticles is shown in Fig. 5 respectively.

4.1.2 Transmission electron micrographs (TEM)

In order to examine size of the gelatin nanoparticles and iron oxide incorporated nanoparticles at nano scale TEM studies were performed. The TEM images shown in Fig. 5a and b reveal that the size of nanoparticles was estimated up to about 100 nm and shape of particles was uniform.

4.1.3 Surface potential measurements

The value of ξ potential for unloaded, Iron oxide loaded and drug loaded nanoparticles are summarized in Table 2 which clearly indicate that upon loading of iron oxide molecules onto the nanoparticle surface a net increase in the positive potential of the particles surface occurs at pH 1.8, 7.4 and 8.6 which can be explain by assuming that adsorption of iron oxide particles occurs over the surface of gelatin nanoparticles and this adsorption of iron oxide particles increase the negative charge over the surface of gelatin nanoparticles which is also confirmed by other coworkers [32]. When iron oxide loaded gelatin nanoparticles dipped into the DOX solution, DOX molecules loaded into the particles surface. The zeta potential of DOX loaded particles summarized in Table 2. The result summarized in table clearly indicate that zeta potential of the DOX loaded particles increased at pH 1.8 whereas a decreased in zeta potential observed at pH 7.4 and 8.6, which can be explained on the basis of structural change of the DOX molecules. As DOX molecule is a amphoteric in nature. At pH 1.8, DOX molecules acquire net positive charge due to formation of NH^{3+}. Due to positive charge on DOX Molecules and negative charge on iron loaded gelatin nanoparticles, DOX molecules attached via electrostatic attraction onto the surface of iron loaded nanoparticles which results in increase of zeta potential. In case of pH 7.4 and 8.6, DOX molecules have either neutral or negative charge. So DOX molecule has fewer tendencies to attach on negatively charged iron loaded gelatin nanoparticles. Therefore, less adsorption of DOX molecule onto the surface of iron loaded gelatin loaded nanoparticles results in decease in zeta potential.

Table 2 Surface potentials of unloaded and loaded gelatin nanoparticles

Particles	Medium (pH)	ξ Potential (mV)
Unloaded nanoparticles	1.8	283
	7.4	−38.4
	8.6	−4.5
Iron oxide loaded nanoparticles	1.8	284.5
	7.4	−40.7
	8.6	−71.8
Drug loaded nanoparticles	1.8	301
	7.4	−34.5
	8.6	−18.6

4.1.4 Magnetization measurements

The magnetic moment of each dried magnetic particles was measured over a range of applied fields between −80000 and +80000 Gauss with a sensitivity of 0.1 emu g^{-1}.

Figure 6 shows a typical magnetization (M) versus the applied magnetic field (H) plot. The saturation magnetization of the synthetic magnetic particles was found to be equal to 25 emu g^{-1} at 300 K. The value obtained is lower than the reported values of 92–100 emu g^{-1} for magnetite (Fe_3O_4) nanoparticles [39] and may be attributed to the fact

that below a critical size, nanocrystalline magnetic particles may be of single domain and show the unique phenomenon of superparamagnetism [40]. A particle of the magnetic material below a critical diameter, depending on the particle material, approximately 8 nm for Fe_2O_3 particles [41], contains only one single magnetic domain, so that this particle is at a state of uniform magnetization at any field without interaction with nieghbour domain in one particle or a well dispersed suspension. In fact, the critical diameter is the single domain size of the materials. Hence, an object consisting of many of these nanosized particles displays magnetic properties under an applied magnetic field, but permanent magnetization would not remain when the applied magnetic field has been removed. The reason for this phenomenon, superparamagnetism, is that these domains will return to disordered status by having enough space to refuse the interaction between each other while there is no extra magnetic field applied.

Magnetization measurements have shown that the saturation magnetization of γ-Fe_2O_3 nanocrystals, small enough to show super paramagnetic properties, decreases with decreasing particle size. However, such reduction is difficult to be interpreted by considering only the finite size and surface effects [42]. To explain this phenomenon several hypotheses, even those concerning the cationic disorder in the entire volume of the crystal structure, have been proposed. There is, however, no unequivocal way for clearly differentiating the individual contributions arising from finite-size, surface effects and structure of the particles. Different magnetic properties have been observed in materials with similar nominal grain-size but produced by different synthetic routes thus making the study of the interrelation between microstructure and magnetism very interesting. A possible explanation is that various syntheses may lead to particles having the same size magnitude order but different structural coherence in the whole particle volume [43]. There is no abrupt breakdown in atomic order, but it is present in a three-dimensional lattice distortion due to the defects and finite size resulting in different magnetization values [44].

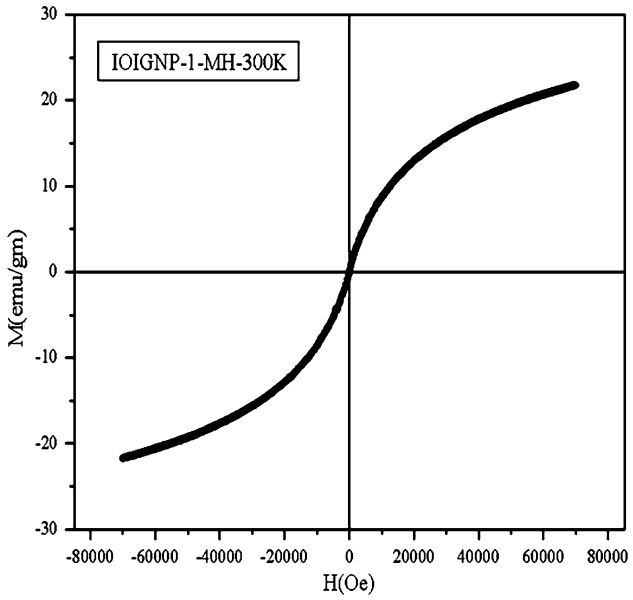

Fig. 6 A typical magnetization (M) versus the applied magnetic field (H) plot for the iron oxide impregnated gelatin nanoparticles

4.1.5 Mechanism of drug release

A swollen particle may be imagined as a three dimensional polymer network structure between the strands of which are present water-filled permeation channels. The water occupies the permeation channels when the water soluble solutes diffuse out to the external receptor medium from within the gel. A free volume theory assumes that the free volume of the water present in the hydrogel is available for the diffusion of water soluble solutes. The theory implies that the free volume in a polymer may be thought of as a volume fraction of molecular size holes available for diffusion. In the present case, the drug carriers are the crosslinked gelatin nanoparticles which in aqueous release medium (pH 7.4) will exist carrying almost equal number of positive ($-NH_3^+$) and negative ($-COO^-$) charges (because pH 7.4 is isoelectric point also). At pH 7.4 the drug (DOX) will also be present in 100% ionized state. Thus, the positively charged DOX molecules may be bound to the negatively charged $-COO^-$ groups via electrostatic attraction. The whole mechanism of DOX release is modeled in Fig. 4.

4.2 Results on doxorubicin (DOX) release

4.2.1 Release experiments

The objectives of the release experiments are to determine the parameters that affect the release of doxorubicin (DOX) The effects of crosslinker, gelatin composition, pH, magnetic material, physiological fluid type of gelatin, presence and absence of magnetic field were studied. The samples were methodically processed after each experiment to make sure that every sample was treated in the same manner for quality of comparison.

4.2.2 Effect of % loading on release of DOX in absence and presence of magnetic field

In the present study, the physical loading was followed which involve swelling of preweighed nanoparticles into the doxorubicin (DOX) solution of concentration ranging from 25.45 to 62.9% (v/v). The loaded nanoparticles were

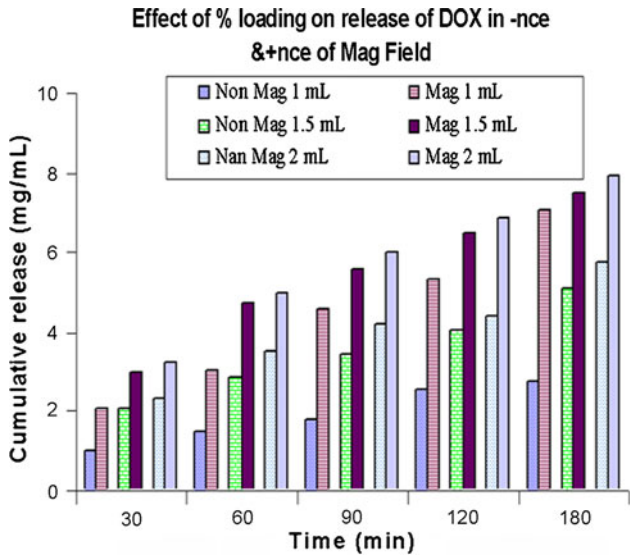

Fig. 7 Effect of %loading of DOX on its release profile for a definite composition of nanoparticles [gelatin] = 5.0 g, [genipin] = 0.1326 mM, pH = 7.4, temp. = 25 ± 0.2°C

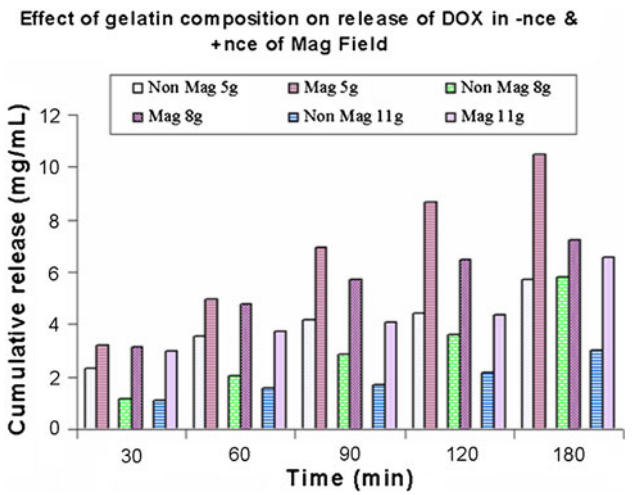

Fig. 8 Effect of varying amounts of gelatin in nanoparticles on release profiles of DOX for a definite composition of nanoparticles [genipin] = 0.1326 mM, pH = 7.4, temp. = 25 ± 0.2°C, %loading = 62.9

allowed to release the entrapped DOX into definite volume of the medium in both presence and absence of magnetic field. The release profiles of nanoparticles loaded to different extent are shown in Fig. 7 which clearly indicate that the released amount of DOX increases with increasing % loading in both cases but in the presence of magnetic field release of dox is comparatively higher. The observed increase in the release rate may be attributed to the fact that a larger loading of the nanoparticles facilitates a faster movement of the invading solvent front (PBS) which as a consequence enhances the release of the entrapped drug.

It is assumed that synthesized IOIGNPs could cause faster movements in the presence of sufficient external magnetic field.

The observed results may be attributed to the fact that the magnetic moment of a material m, is proportional to the applied field H (according to Eq. 3).

$$M = \chi m\ H \tag{3}$$

where χm is magnetic susceptibility of the material. When loaded nanoparticles are exposed to a high magnetic field, magnetic monodomain nanoparticles generates heat through oscillation of magnetic moments and subsequently enlarges the nanostructure of the polymeric matrix to produce porous channels that cause enhanced diffusion process and as a consequence the drug to be released easily. The mechanical deformation generates compressive and tensile stresses, enhancing the release of DOX. Similar types of results have also been reported elsewhere [45]. It is important to mention here that although in the present case direct current (DC) was used to produce magnetic field, however, since the drug containing nanoparticles were in constant and rapid motion, they were experiencing rapidly changing magnetic field and due to this fluctuation the magnetic nanoparticles produced friction within the matrix and result in loosening of the network chains of gelatin.

4.3 Effect of composition on DOX release

4.3.1 Effect of gelatin composition on release of DOX in absence and presence of magnetic field

Drug release profiles are often sensitive to chemical architecture of the carrier as well as the experimental conditions of preparation of drug carrier. In the present study too, the size and morphology of nanoparticles are greatly determined by the factors such as amounts of gelatin and genipin in the feed mixture, molecular weight of PMMA and temperature and shaking time of emulsions.

The effect of gelatin on the DOX release has been investigated by varying its amount in the range 5.0–11.0 g in the feed composition. The release results in the presence and absence of magnetic fields are shown in Fig. 8 which clearly indicate that the cumulative release of doxorubicin (DOX) decreases with increasing concentration of gelatin up to 11.0 g in both the conditions.This decrease is due to the fact that when the amount of gelatin is low at fixed crosslinker concentration, the nanoparticles produced have greater porosity due to increased number of crosslink per gelatin molecule. In this way greater numbers of pores are available for entrance of water molecules and release of the drug. This will obviously result in an increased release.

4.3.2 *Effect of crosslinker composition on release of DOX in absence and presence of magnetic field*

Certain reagents have been used for crosslinking chitosan such as glutaraldehyde, tripolyphosphate, ethylene glycol, diglycidyl ether and diisocyanate. However, studies have shown that the synthetic crosslinking reagents are more or less cytotoxic and may impart the biocompatibility to the chitosan delivery system. Hence, it is desirable to provide a good crosslinking reagent for their use in biomedical applications that has low cytotoxicity and forms stable and biocompatible crosslinked products.

Besides the empirical data of the traditional medicine, today some information on the beneficial effects of genipin is available in biochemical terms [46]. Used gardenia for the treatment of liver cirrhosis and their investigation showed that the activated hepatic stellate cells could be suppressed by genipin. Genipin reveals remarkable effects as an anti-inflammatory and anti-angiogenesis agent, and inhibits lipid peroxidation and production of nitric oxide, besides protecting the hippocampal neurons from the toxicity of Alzheimer's amyloid beta protein it was found that genipin protected mice from the lethal effect of administered GalN-LPS: in fact 8 out of 15 mice survived for at least 24 h, whilst all mice not given genipin died within 12 h [47, 48]. In mice given genipin, serum and liver tumor necrosis factor-alpha levels as well as serum AST and ALT activities were significantly lower; hepatic necrosis and inflammatory cells infiltration were slight. TNF-a, NF-jB activation and TNF-a mRNA expression in the cultured mouse macrophage-like cell line J774.1 were significantly suppressed by genipin administration. Therefore genipin was a remedy for acute hepatic dysfunction thanks to its suppressive effect on TNF-a production.

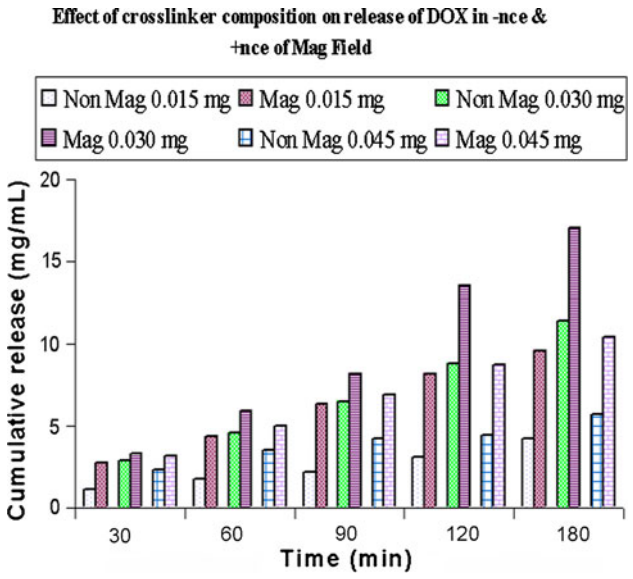

Fig. 9 Effect of varying amounts of genipin (crosslinker) on release profiles of DOX for a definite composition of nanoparticle [gelatin] = 5.0 g, pH = 7.4, temp. = 25 ± 0.2°C, %loading = 62.9

The effect of crosslinker on the release profiles of DOX of an applied magnetic field has been investigated by varying the concentration of genipin in the range 0.0663–0.1989 mM. The results are shown in Fig. 9, which clearly reveal that the cumulative release of DOX increase with increasing genipin up to 0.1326 mM concentration while beyond it a fall in release is noticed. The results can be explained by the fact that since genipin is a hydrophilic cross linker, its increasing number of linkages in the nanoparticles enhances their hydrophilicity which, in turn, will allow increasing number of water molecules into the nanoparticles and obviously the swelling ratio will increase. Thus, increased swelling will permit greater number of DOX molecules to diffuse out and the release of DOX will also increase.

It is, however, noticed that beyond 0.1326 mM of genipin, the size of nanoparticles will decrease due to enhanced crosslinking density of the nanoparticles and as a result; both swelling and the drug release will fall.

Another explanation for the observed decrease in the swelling ratio and DOX release may be that increasing the crosslinker concentration lowers the molecular weight between crosslink and this, consequently, reduces the free volume accessible to the penetrant water molecules. Similar types of results have also been reported by other workers [49]. Some authors [50] however, have reported that introduction of cross linker into the polymer matrix enhances its glass transition temperature (T_g) which because of glassy behavior of polymers restrains the mobility of network chains and, therefore, both swelling and DOX release decrease.

4.3.3 *Effect of pH on DOX release in absence and presence of magnetic field*

In the present investigation, the release dynamics of the DOX has been observed under varying pH conditions as found in the GIT [e.g., stomach (gastric juice) 1.0, and small intestine 7.5–8.6]. The wide range of pH allows a specific drug to be delivered to a targeted site only. For example, the pH in the stomach (<3) is quite different from the neutral pH in the intestine and this pH difference could be used to prevent release of foul-tasting drugs into the neutral pH environment of the mouth while using polycationic hydrogels as drug carrier [51]. Similarly, a polyanion hydrogel which shows a minimal swelling in acidic pH (such as in stomach) could be of potential use to increase in pH leading to ionization of the carboxylic groups [52].

The drug-release kinetics for Dox IOIGNP was studied at three different pH conditions Fig. 10. It is observed that

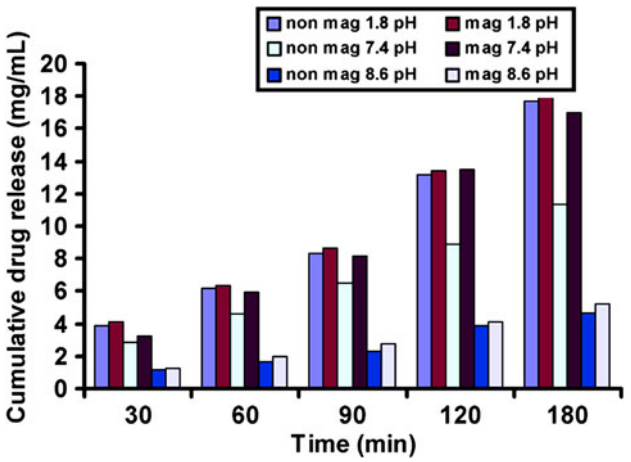

Fig. 10 Variation in released amount of DOX with varying pH of the release medium for a definite composition of nanoparticle [gelatin] = 5.0 g, [genipin] = 0.1326 mM, temp. = 25 ± 0.2°C, %loading =62.9

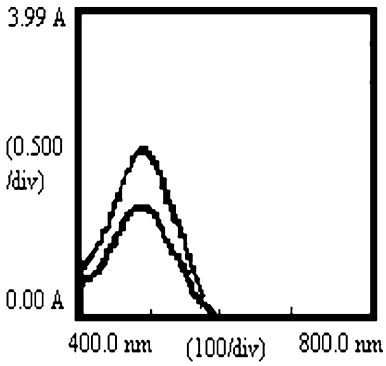

Fig. 11 UV spectra showing the chemical stability of doxorubicin in its **a** pure solution, **b** released medium

Dox release would be faster at acidic pH values than at basic pH as a consequence of weakened binding between Dox and the partially neutralized car boxy groups in IO-IGNP. This is due to the fact that the physically bound drug molecules could be released faster in the mild acidic environments of tumor areas than at the physiologically neutral pH of blood in the vascular compartment.

4.3.4 Chemical stability of drug

In order to ascertain the chemical stability of DOX in highly acidic pH medium such as gastric juice, the drug was left in simulated gastric juice medium and its UV spectra was scanned and compared to that of DOX in the aqueous medium. The spectra are shown in Fig. 11 which clearly indicate that they are almost identical to each other. This obviously suggests that even in remaining in highly acidic media, the chemical nature of DOX does not change.

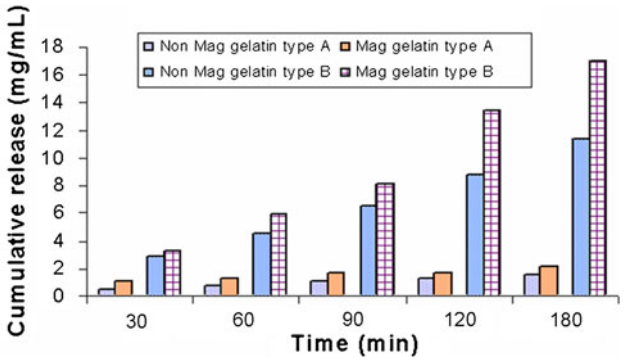

Fig. 12 Effect of type of gelatin on the released amount of DOX for definite compositions of nanoparticle [gelatin] = 5.0 g, [genipin] = 0.1326 mM, pH = 7.4, temp. = 25 ± 0.2°C, %loading = 62.9

Moreover, it was also found that even gelatin nanoparticles do not undergo any cleavage in gastric juice medium. This clearly explains the stability of drug carrier system in highly acidic media.

4.3.5 Effect of type of gelatin on release of DOX in absence and presence of magnetic field

Gelatin is a natural polymer that is extracted from collagen by alkaline or acidic pretreatment and thermal denaturation [53]. Depending on this pretreatment two types of gelatin can be distinguished, A and B. Gelatin A is extracted from porcine skin, and processed by acidic pretreatment, while gelatin B is extracted from bovine skin, and processed by alkaline pretreatment. The alkaline pretreatment converts glutamine and aspargine residues into glutamic acid and aspartic acid, which results in a higher carboxylic acid content for gelatin B (118/1000 amino acids) than for gelatin A (77/1000 amino acids) [54].

The effect of type of gelatin on the release profile of DOX in presence and absence of magnetic field has been investigated by loading the drug onto both gelatin A and B nanoparticles and following the released amounts under identical experimental conditions. The results are shown in Fig. 12 which clearly indicates that the cumulative release of drug is quite higher in case of type B than that by type A. The results may be explained by the fact that at the experimental pH (7.4) (which is above the isoelectric point 4.8 of gelatin) the gelatin B molecules will possess a net negative charge due to $-COO^-$ groups in the molecule. Thus, the DOX molecules, which are almost fully ionized at pH 7.4, will attach to these negatively charged centers present along the gelatin molecules and, therefore, will result in a greater percent loading. When largely loaded type B nanoparticles are placed in the release medium the $-COO^-$ groups present along the gelatin chains repel each other, thus producing a greater relaxation in the

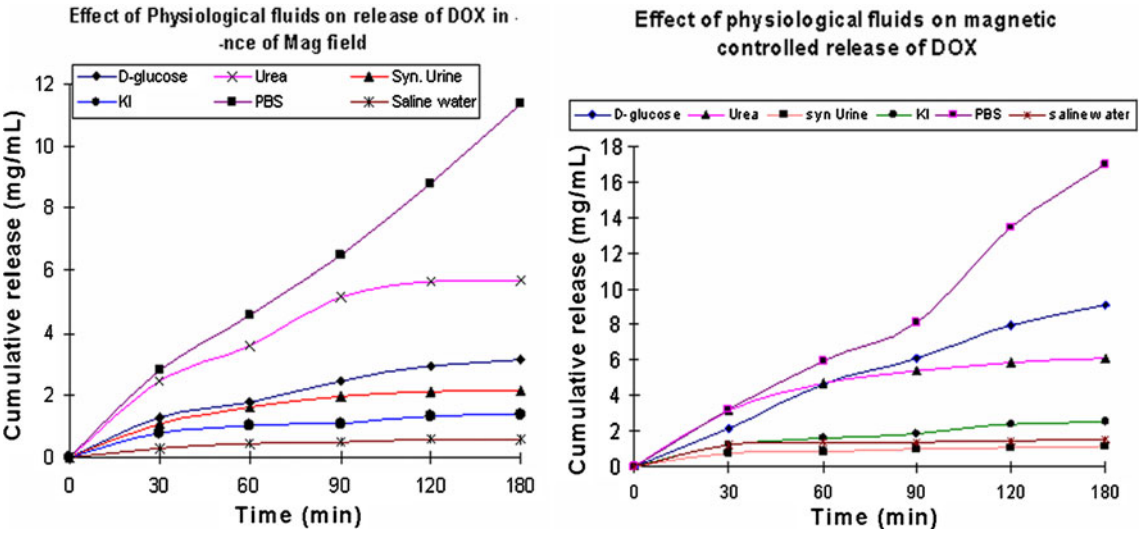

Fig. 13 Effect of physiological fluids on the released amount of DOX for definite composition of nanoparticle [gelatin] = 5.0 g, [genipin] = 0.1326 mM, pH = 7.4, temp. = 25 ± 0.2°C, %loading = 62.9

nanoparticles. This obviously results in a larger swelling of the loaded nanoparticles which, in turn, produces greater release of DOX in type B nanoparticles. Similar types of results have also been published elsewhere [55].

4.3.6 Effect of physiological fluid on DOX Release absence and presence of magnetic field

The effect of nature of the medium on the release kinetics of DOX in presence and absence of magnetic field has been investigated by performing release experiments in various physiological fluids. The results are depicted in Fig. 13 which reveals that the release of DOX in both conditions is significantly suppressed in physiological fluids in comparison to that in the PBS. The possible reason for the lower release and swelling of DOX in these fluids may be that the presence of salt ions in the release medium lowers the rate of penetration of water molecules into the loaded nanoparticles, thus resulting in a fall in the release amount of. DOX In the case of urea, its capacity to break hydrogen bonds between water molecules and IPN chains may be responsible for the lower amount of water uptake [56] and consequently for the lower release of DOX.

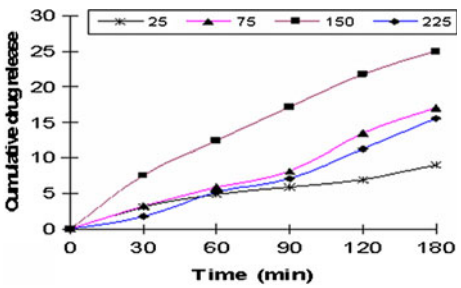

Fig. 14 Effect of magnetic field on the released amount of DOX for definite compositions of nanoparticle [gelatin] = 5.0 g, [genipin] = 0.1326 mM, pH = 7.4, temp. = 25 ± 0.2°C, %loading = 62.9

4.3.7 Effect of magnetic field strength on DOX release

The release results are shown in Fig. 14 clearly indicate that the cumulative release of doxorubicin (DOX) increases with increasing magnetic field strength up to 150 gauss while beyond it a fall in release is noticed. The initial increase observed in the released drug with increasing magnetic field up to 150 gauss may be due to increase in mechanical stress within the nanoparticles matrix as explained earlier also. However, beyond 150 gauss, the walls between the macropores in the magnetic particle network of the ferrosponge possess large amounts of mesopores, in which drug release is solely dominated by molecular diffusion through the mesopores to environment. By magnetizing the iron oxide nanoparticles in the walls, the mesopores size decreases considerably, this restricted more effectively the diffusion of the drug molecules. Consequently, the drug release rates decreased immediately while applying an external magnetic field. The interaction between magnetic particles has been demonstrated to occur under an external magnetic field [57].

5 Conclusions

Genipin crosslinked gelatin nanoparticles form a swelling controlled drug release system, which effectively delivers doxorubicin in the presence and absence of magnetic field via diffusion controlled pathway.

It is found that release profiles of DOX are greatly influenced by % loading of DOX, concentrations of gelatin and genipin (cross linker) in the nanoparticles. It is noticed that with increase in percent loading of drug, the released amount of DOX constantly increases.

In the case of gelatin, the release of DOX decreases when the amount of gelatin is increased from 5.0 to 11.0 g whereas the extent of release decreases beyond 5.0 g of gelatin content. The released amount of DOX increases with increasing genipin content up to 0.1326 mM whereas the extent of release decreases beyond 0.1326 mM of genipin content.

It is observed that the release behavior is directly regulated by the extent of swelling of gelatin nanoparticles. Type of gelatin also has a profound effect on the release potential of nanoparticles and it is found that type B gelatin nanoparticles show a greater drug delivery than that by type A nanoparticles.

The chemical stability of DOX suggests that even in remaining in highly acidic media, the chemical nature of DOX does not change. The zeta potential of the DOX loaded particles increased at pH 1.8 whereas a decreased in zeta potential observed at pH 7.4 and 8.6.

An optimum drug release is obtained at acidic pH while lower release is observed in basic pH range. The physiological fluids suppress the extent of release of. DOX.

Acknowledgments The authors acknowledge the Department of Science & Technology, New Delhi, India for awarding Women Scientist Fellowship to one of the authors (Dr. Jyoti Choubey) and IUC-DAE, Indore (M.P.) for performing magnetization study.

References

1. Lubbe AS, Alexiou C, Bergemann C. Clinical applications of magnetic drug targeting. J Surg Res. 2001;95:200–6.
2. Widder KJ, Morris RM, Poore GA, Howards DP, Senyei AE. Selective targeting of magnetic albumin microspheres containing-dose doxorubicin: total remission in Yoshida sarcoma-bearing rats. Eur J Cancer Clin Oncol. 1983;19:135–9.
3. Alexiou C, Arnold W, Klein RJ, Parak FG, Hulin P, Bergemann C, et al. Experimental therapeutics locoregional cancer treatment with magnetic. Drug Target Cancer Res. 2000;60:6641–8.
4. De Paoli VM, De Paoli Lacerda SH, Spinu L, Ingber B, Rosenzweig Z, Rosenzweig N. Effect of an oscillating magnetic field on the release properties of magnetic collagen gels. Langmuir. 2006;22(13):5894–9.
5. Lu ZH, Prouty MD, Guo ZH, Golub VO, Kumar CSSR, Lvov YM. Magnetic switch of permeability for polyelectrolyte microcapsules embedded with Co@Au nanoparticles. Langmuir. 2005;21(5):2042–50.
6. Rana S, Gallo A, Srivastava RS, and Misra RD. On the suitability of nanocrystalline ferrites as a magnetic carrier for drug delivery: functionalization, conjugation and drug release kinetics. Acta Biomater. 2007;3(2):233–42.
7. Edelman ER, Kost J, Bobeck H, Langer R. Regulation of drug release from polymer matrices by oscillating magnetic fields. J Biomed Mater Res. 1985;19(1):67–83.
8. Wilhelm C, Cebers A, Bacri JC, Gazeau F. Deformation of intracellular endosomes under a magnetic field. Eur Biophys J. 2003;32(7):655–60.
9. Horak D, Lednicky F, Petrovsky E, Kapicka A. Magnetic characteristics of ferrimagnetic microspheres prepared by dispersion polymerization. Macromol Mater Eng. 2004;289(4):341–8.
10. Leach JH (2002) Magnetic targeted drug delivery. MSc Thesis, Department of Electrical Engineering, Virginia Tech
11. Harris LA, Goff JD, Carmichael AY, Riffle JS, Harburn JJ. Magnetite nanoparticles dispersions stabilized with triblock copolymers. Chem Mater. 2003;15:1367–77.
12. Gu H, Xu K, Yang Z, Chang CK, Xu B. Synthesis and cellular uptake of porphyrin decorated iron oxide nanoparticles-a potential candidate for bimodal anticancer therapy. Chem Commun (Camb). 2005;34:4270–2.
13. Thomson RC, Yaszemski MJ, Powers JM, Mikos AG. Fabrication of biodegradable polymer scaffolds to engineer trabecular bone. J Biomater Sci Polym Ed. 1995;7(1):23–38.
14. Khan A, Benboubetra M, Sayyed PZ, Ng KW, Fox S, Beck G, et al. Sustained polymeric delivery of gene silencing antisense ODNs, siRNA, DNAzymes and ribozymes: invitro and in vivo studies. J Drug Target. 2004;12(6):393–404.
15. Li Z, Huang L. Sustained delivery and expression of plasmid DNA based on biodegradable polyester, poly (D, L-lactide-co-4-hydroxy-L-proline). J Control Release. 2004;98(3):437–46.
16. Ahlin P, Kristl J, Kristl A, Vrecer F. Investigation of polymeric nanoparticles as carriers of enalaprilat for oral administration. Int J Pharm. 2002;239(1–2):113–20.
17. Yang J, Lee H, Hyung W, Park SB, Haam S. Magnetic PECA Nanoparticles as drug carriers for targeted delivery: synthesis and release characteristics. J Micro encapsul. 2006;23(2):203–12.
18. Elvira C, Fanovich A, Fernandez M, Fraile J, San Roman J, Domingo C. Evaluation of drug delivery characteristics of microspheres of PMMA-PCL-cholesterol obtained by supercritical-CO2 impregnation and by dissolution-evaporation techniques. J Control Release. 2004;99(2):231–40.
19. Owais M, Gupta CM. Targeted drug delivery to macrophages in parasitic infections. Curr Drug Deliv. 2005;2(4):311–8.
20. Chan LW, Liu X, Heng PW. Liquid phase coating to produce controlled release alginate microspheres. J Microencapsul. 2005;22(8):891–900.
21. Young S, Wong M, Tabata Y, Mikos G. Gelatin as a delivery vehicle for the controlled release of bioactive molecules. J Control Release. 2005;109:256–74.
22. Kushibiki T, Tomoshige R, Fukunaka Y, Kakemi M, Tabata Y. In vivo release and gene expression of plasmid DNA by hydrogels of gelatin with different cationization extents. J Control Release. 2003;90:207–16.
23. Liang H-C, Chang W-H, Lin K-J, Sung H-W. Research article genipin-crosslinked gelatin microspheres as a drug carrier for intramuscular administration: in vitro and in vivo studies. J Biomed Mater Res Appl Biomater. 2003;65A(2):271–82.
24. Dunkan R, Dimitoijevic S, Evagaron EG. STP Pharma. Sci. 1996;6:237.
25. Lefrak EA, Ritha J, Rosenheim S. A clinicopathologic analysis of adriamycin cardiotoxicity. Cancer. 1973;32:302–14.
26. Couvreur P, Kante B, Grislain L, Roland M, Speiser P. Toxicity of polyalkylcyanoacrylate nanoparticles II: doxorubicin-loaded nanoparticles. J Pharm Sci. 1982;71:790–2.
27. Callister WD Jr. Materials science and engineering—an introduction. 5th ed. New York: Wiley; 2000.
28. Inan US, Inan AS. Engineering electromagnetics. New York: Addison-Wesley; 1999.
29. Voltairas PA, Fotiadis DI, Michalis LK. Hydrodynamic of magnetic drug delivery. J Biomech. 2002;35:813–21.

30. Murakami H, Kawashima Y, Niw T, Hin T, Takeuchi H, Kobayashi M. Influence of the degrees of hydrolyzation and polymerization of poly(vinylalcohol) on the preparation and properties of poly(DL-lactide-co-glycolide) nanoparticles. Int J Pharm. 1997;149:43–9.
31. Le Ray AM, Vert M, Gautier JC, Benoit JP. End-chain radiolabeling and in vitro stability studies of radiolabeled poly(hydroxy acid) nanoparticles. J Pharm Sci. 1994;83:845–51.
32. Illes E, Tombacz E. The effect of humic acid adsorption on pH-dependent surface charging and aggregation of magnetite nanoparticles. J Colloid Interface Sci. 2006;295:115–23.
33. Shi Y, Moog C. Carboxyl group(-COOH) functionalized ferromagnetic iron oxide nanoparticles for potential bio-applications. J Mater Chem. 2004;14:2781–6.
34. Skoeld RO, Mats AR. Adsorption of bis(triethanolammonium) 1,10-decanedicarboxylate on magnetite from aqueous solution. Tunius Langmuir. 1994;10(1):211–17.
35. van de Weert M, Haris PI, Hennink WE, Crommelin DJ. Fourier transform infrared spectrometric analysis of protein conformation: effect of sampling method and stress factors. Anal Biochem. 2001;297(2):160–9.
36. Davidson GWR, Peppas NA. Solute and penetrant diffusion in swellable polymer. V. Relaxation controlled transport in P (HEMA-co-MMA) copolymers. J Control Release. 1986;3:243.
37. Wang A, Li–Fang, Chen, WB, Tzu–Yichen and Shui Chunlu (2003) J Biomater Sci Polymer Edn 14(1):27.
38. Zhong ZY, Prozorov T, Felner I, Gedanken A. Sonochemical synthesis and characterizationof iron oxide coated on submicrosphrical alumina: a direct observation of interaction between iron oxide and alumina. J Phys Chem B. 1999;103:947–56.
39. Morales MA, Jain TK, Labhasetwar V. Magnetic studies of iron oxide nanoparticles coated with oleic acid and pluronic® block copolymer. J Appl Phys, 2005; 97:10Q905-3.
40. Chia CH, Zakaria S, Ahamd S, Abdullah M, Mohd JS. Preparation of magnetic paper from kenaf: lumen loading and in situ synthesis method. Am Appl Sci. 2006;3:1750–4.
41. Schmidt H. Nanoparticles by chemical synthesis, processing to materials and innovative applications. Appl Organometal Chem. 2001;15:331–43.
42. Morales MP, Veintemillas-Verdaguer S, Montero MI, et al. Surface and internal spin canting in–Fe2O3 nanoparticles. Chem Mater. 1999;11:3058–64.
43. Serna CJ, Bodker F, Morup S, et al. Spin frustration in maghemite nanoparticles. Solid State Commun. 2001;118:437–40.
44. Di Marco M, Port M, Couvreur P, et al. Structural characterization of ultrasmall superparamagnetic iron oxide (USPIO) particles in aqueous suspension by energy dispersive X-ray diffraction (EDXD). J Am Chem Soc. 2006;128:10054–9.
45. Shang-Hsiu Hu, Ting-Yu Liu, Hsin-Yang Huang, Dean-Mo Liu, San-Yuan Chen. Magnetic-sensitive silica nanospheres for controlled drug release. Langmuir. 2008;24(1):239–44.
46. Mie I, Satoshi M, Atsushi M, Kenji F. Japanese herbal medicine inchin-koto as a therapeutic drug for liver fibrosis. J Hepathol. 2004;41:584–91.
47. Koo HJ, Song YS, Kim HJ, Park EH. Anti-inflammatory effects of genipin, an active principle of gardenia. Eur J Pharmacol. 2004;495:201–8.
48. Takeuchi S, Goto T, Mikami KI, Miura K, Ohshima S, Yoneyama K, et al. Genipin prevents fulminant hepatic failure resulting in reduction of lethality through the suppression of TNF-alpha production. Hepatol Res. 2005;33(4):298–305.
49. Cohn D, Aronhime M, Abdo B. Poly (Urethane)-crosslinked poly(HEMA) hydrogels. J Macromol Sci Pure Appl Chem. 1992;29A:841–51.
50. Ramaraj B, Radhakrishnan G. Modification of the dynamic swelling behavior of poly(2-hydroxyethyl methacrylate) hydrogels in water through interpenetrating polymer network. Polymer. 1994;35:2167–73.
51. Qiu Y, Park K. Environment sensitive hydrogels for drug delivery. Adv Drug Deliv Rev. 2001;53(3):321–39.
52. Bilia A, Carelli V, Colo GD, Nannipieri E. In vitro evaluation of a ph sensitive hydrogel for control of GI drug delivery from silicon-base matrices. Int J Pharm. 1996;130(1):83–92.
53. Rose PI. Encyclopedia of polymer science and engineering. New York: John Wiley; 1987. p. 488–513.
54. Johns P, Courts A. Relationship between collagen and gelatin. In: Ward AG, Courts A, editors. The science and technology of gelatin. London: Academic Press; 1977. p. 138–77.
55. Kuijpers AJ, Engbers GHM, van Wachem PB, Krijgsveld J, Zaat SAJ, Dankert J, et al. Controlled delivery of antibacterial proteins from biodegradable matrices. J Controlled Rel. 1998;53:235–47.
56. Nosaka AY, Tanzawa HJ. H-NMR studies on water in methacrylate hydrogels. J Appl Polym Sci. 1991;43(6):1165.
57. Hu S-H, Liu T-Y, Liu D-M, Chen S-Y. Nano-ferrosponges for controlled drug release. J Controlled Release. 2007;121(3):181–9.